Strain-polarization coupling in the Low-Dimensional van der Waals Ferrielectrics

*Note: Sub-titles are not captured in Xplore and should not be used

Anna N. Morozovska
Institute of Physics
National Academy of Sciences of Ukraine
Kyiv, Ukraine
anna.n.morozovska@gmail.com

Hanna V. Shevliakova
Department of Microelectronics
National Technical University of Ukraine "Igor Sikorsky Kyiv Polytechnic Institute"
Kyiv, Ukraine
shevliakova.hv@gmail.com

Liubomyr M. Korolevych
Department of Microelectronics
National Technical University of Ukraine "Igor Sikorsky Kyiv Polytechnic Institute"
Kyiv, Ukraine
korolevych.lyubomyr@gmail.com

Victoria Khist
[1)] Department of General Physics
National Technical University of Ukraine "Igor Sikorsky Kyiv Polytechnic Institute"
[2)] Department of Physics of Meso- and Nanocrystalline Magnetic Structures
Institute of Magnetism
NAS of Ukraine and MES of Ukraine
Kyiv, Ukraine
khist2012@gmail.com

Yulian M. Vysochanskii
Institute of Solid State Physics and Chemistry, Uzhhorod University, 88000 Uzhhorod, Ukraine
vysochanskii@gmail.com

Eugene A. Eliseev
Institute for Problems of Materials Science
National Academy of Sciences of Ukraine
Kyiv, Ukraine
eugene.a.eliseev@gmail.com

***Abstract*— Using the Landau-Ginzburg-Devonshire phenomenological approach we explore the strain-polarization coupling in the low-dimensional van der Waals ferrielectrics. We evolve the analytical model of the piezoelectric susceptibility of the material in response to the periodic strain modulation, such as caused by a surface acoustic wave. Numerical calculations are performed for recently discovered and poorly studied ultrathin layers of vdW ferrielectric $CuInP_2S_6$, which are very promising candidates for advanced nanoelectronics.**

Keywords*— *van der Waals ferrielectrics, $CuInP_2S_6$, strain-polarization coupling, piezoelectric susceptibility

I. Introduction

Two-dimensional van der Waals (vdW) materials, the first representative of which is graphene, have long been of interest to researchers [1]. A unique feature of vdW materials is the strong interatomic bonds within the monolayer, and weaker van der Waals forces between the layers. Thanks to this, they can be divided into single-layer (SL) structures. Due to the van der Waals forces between the layers, these materials are convenient for the creation of heterostructures based on them since the formation due to van der Waals forces does not require agreement in lattice constants. VdW materials have significant differences between out-of-plane and in-plane properties, and the properties of sing-layer (SL) and their bulk materials, or even 2- or 3-layer structures, it is clearly can be shown with an example of low-dimensional (LD) transition metal dichalcogenides (TMDs). Tunability of polar and semiconducting properties of LD-TMDs with a chemical formula MX_2 (M – metal Mo, W, Re; X – chalcogen S, Se, Te) [2, 3] and Janus-compounds (JC) with a chemical formula MXY (X, Y – chalcogens) [4, 5, 6] came them to the forefront of fundamental and applied physical research.

A very interesting representative of vdW materials is a Copper indium thiophosphate (CIPS), with chemical formula $CuInP_2S_6$, not only because of its vdW structure, but also the presence of reliable out-of-plane ferroelectricity at temperatures close to the room [7]. Its unique ferroelectric properties are largely induced by Cu off-centering (Fig. 1b) [8]. Also, the negative capacitance of CIPS was detected, which allows to improve the control of the current in the channel of the field-effect transistors (FETs), thereby reducing power consumption and heating [9]. Therefore, due to the variety of its unique properties, CIPS has a wide range of applications in ferroelectric non-volatile random-access memory (FRAM) [10] and ferroelectric FET (Fe-FETs) [11].

The presence of spontaneous polarization immediately arouses interest in the study of other polar properties of these materials, such as piezoelectric [12, 13], electrocaloric and pyroelectric [14] effects, thanks to which they can be used in pyroelectric nanogenerator [15] and solid-state cooling devices [16], in piezoelectric and straintronic devices [17], and ultrasound transducers [18].

Despite the fact that many works are devoted to the study of CIPS, many aspects of its piezoelectric and elastic properties are not sufficiently studied and require additional analysis. The knowledge gap motivated this study, devoted to the Landau-Ginzburg-Devonshire (LGD) phenomenological description of the strain-polarization coupling in the low-dimensional vdW ferrielectrics. Below we present the analytical model of the piezoelectric susceptibility of the vdW material in response to the periodic strain modulation, such as caused by a surface acoustic wave (SAW). Numerical calculations are performed for a CIPS layer.

II. Landau-Ginzburg-Devonshire Approach

The considered structure of CIPS (a-b) and the schematic model of metal-ferroelectric-semiconductor FET (MFS-FET) (c) is shown in Fig. 1.

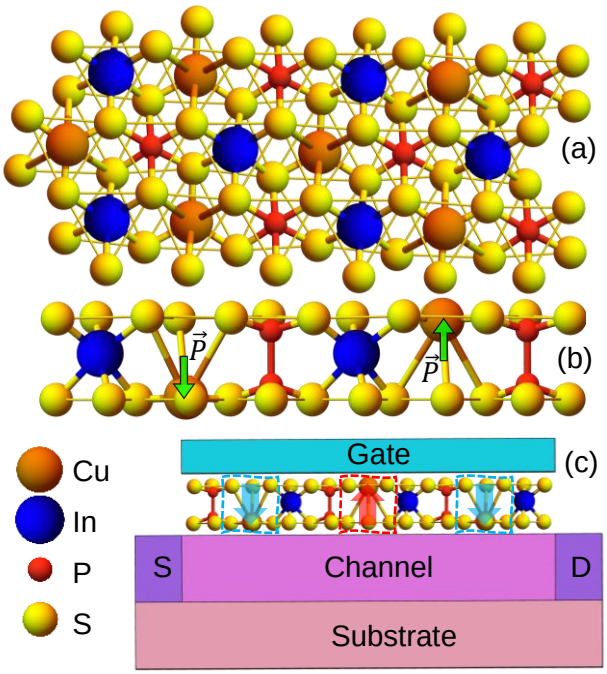

Fig. 1. Top (a) and side (b) view of $CuInP_2S_6$ (CIPS) structure and MFS-FET transistor with a CIPS ferroelectric gate (c). Thanks to CIPS, the channel can be made of wdW material in semiconductor phase, e.g. LD-TMDs.

The bulk density of the LGD free energy F, which depends on polarization component P and strain component u, and their gradients, has the following form [12-14, 19]:

$$F = \frac{\alpha}{2}P^2 + \frac{\beta}{4}P^4 + \frac{\gamma}{6}P^6 + \frac{\delta}{8}P^8 + \frac{g}{2}\left(\frac{\partial P}{\partial x}\right)^2 - quP^2 - zuP^4 - \\ -\frac{f}{2}\left(P\frac{\partial u}{\partial x} - u\frac{\partial P}{\partial x}\right) + \frac{c}{2}u^2 - PE - NU. \qquad (1)$$

According to Landau theory [20, 21], the coefficient α linearly depends on the temperature T for proper ferroelectrics, $\alpha(T) = \alpha_T(T - T_C)$, where T_C is the Curie temperature. All other coefficients in Eq.(1) are supposed to be temperature independent. The condition $\delta \geq 0$ is required for the stability of the free energy for all P values. The gradient positive coefficient g determines the magnitude of the gradient energy. Coefficient f is the component of the static flexocoupling tensor. The elastic stiffness c should be positive for the functional stability. The linear and nonlinear electrostriction coefficients, q and z, can be positive or negative. The elastic displacement component U is related with the strain u as $u = \partial U/\partial x$. N is the bulk density of external mechanical force (e.g., periodic adhesion force induced by a patterned substrate).

The polarization interacts with an external electric field E. We did not include the term $PE_d/2$ in Eq.(1) assuming that the depolarization field E_d is small due to the high conductivity of CIPS, or absent for the in-plane polarization orientation. The absence of E_d corresponds to the transverse fluctuations of polarization, which we consider, and regard that the longitudinal fluctuations of polarization are much smaller due to the depolarization field [22].

The explicit form of the Euler-Lagrange type equations, $\delta F/\delta U = N$ and $\delta F/\delta P = 0$, are:

$$-c\frac{\partial^2 U}{\partial x^2} - f\frac{\partial^2 P}{\partial x^2} + 2qP\frac{\partial P}{\partial x} + 4zP^3\frac{\partial P}{\partial x} = N, \qquad (2a)$$

$$\alpha P + \beta P^3 + \gamma P^5 + \delta P^7 - g\frac{\partial^2 P}{\partial x^2} - f\frac{\partial^2 U}{\partial x^2} - 2qP\frac{\partial U}{\partial x} - \\ -4zP^3\frac{\partial U}{\partial x} = E. \qquad (2b)$$

The integral Fourier transform for polarization is:

$$P = P_S + \int dk \exp(ikx)\,\tilde{P},$$

where P_S is the spontaneous polarization, and k is the wave vector of the SAW.

The integral Fourier transform for elastic displacement is:

$$U = (u_S + u_m)x + \int dk \exp(ikx)\,\tilde{U},$$

where u_S is the electrostriction-induced spontaneous strain, $u_S = \frac{1}{c}(qP_S^2 + zP_S^4)$, and u_m is the misfit strain. In a general case the expression for u_S follows from the equation of state, $\delta F/\delta u = \sigma$.

The integral Fourier transform for perturbating electric field is:

$$E = \int dk \exp(ikx)\,\tilde{E},$$

and the integral Fourier transform for perturbation elastic force density:

$$N = \int dk \exp(ikx)\,\tilde{N}.$$

Using the above Fourier transformations in the linearized Euler-Lagrange Eqs.(2), we obtain the equations for the Fourier images of polarization $\tilde{P}$ and displacement $\tilde{U}$:

$$ck^2\tilde{U} + (fk^2 + 2ikqP_S + 4ikzP_S^3)\tilde{P} = \tilde{N}, \qquad (3a)$$

$$\big(\alpha - 2q(u_S + u_m) + 3\big(\beta - 4z(u_S + u_m)\big)P_S^2 + 5\gamma P_S^4 + \\ +7\delta P_S^6 + gk^2)\tilde{P} + (fk^2 - 2iqkP_S - 4izkP_S^3)\tilde{U} = \tilde{E}. \qquad (3b)$$

The linearized solution of the linearized equations (3) for the polarization has the form:

$$\tilde{P} = \tilde{\chi}(k)\tilde{E} + \tilde{\eta}(k)\tilde{N}. \qquad (4)$$

The linear susceptibilities, $\tilde{\chi}(k)$ and $\tilde{\eta}(k)$, introduced in Eq.(4), are given by the expressions:

$$\tilde{\chi}(k) = \frac{ck^2}{(\alpha_S + gk^2)ck^2 - (fk^2)^2 - (2qP_S + 4zP_S^3)^2k^2},$$

$$\tilde{\eta}(k) = \frac{-(fk^2 - 2iqkP_S - 4izkP_S^3)}{(\alpha_S + gk^2)ck^2 - (fk^2)^2 - (2qP_S + 4zP_S^3)^2k^2}.$$

Here the positive temperature-dependent dielectric stiffness is introduced:

$$\alpha_S(T) = \alpha(T) - 2q(u_S + u_m) + 3\big(\beta - 4z(u_S + \\ +u_m)\big)P_S^2(T) + 5\gamma P_S^4(T) + 7\delta P_S^6,$$

Elastic displacement acquires the explicit form:

$$\tilde{U} = \tilde{\lambda}(k)\tilde{E} + \tilde{\vartheta}(k)\tilde{N}. \quad (5)$$

The linear compliances, $\tilde{\lambda}(k)$ and $\tilde{\vartheta}(k)$, introduced in Eq.(5), are given by the expressions:

$$\tilde{\lambda}(k) \equiv \tilde{\eta}^*(k) = \frac{-(fk^2 + 2ikqP_S + 4izkP_S^3)}{(\alpha_S + gk^2)ck^2 - (fk^2)^2 - (2qP_S + 4zP_S^3)^2 k^2},$$

$$\tilde{\vartheta}(k) = \frac{\alpha_S + gk^2}{(\alpha_S + gk^2)ck^2 - (fk^2)^2 - (2qP_S + 4zP_S^3)^2 k^2}.$$

From the singularity of the generalized susceptibility, corresponding to zero points of the denominator in Eq.(3), we derived the characteristic equation for the transition point:

$$\alpha_S(T)c + (cg - f^2)k^2 - [2qP_S(T) + zkP_S^3(T)]^2 = 0. \quad (6)$$

Fig. 2 and **Fig. 3** illustrate that the dependence of the linearized solution for effective dielectric susceptibility $\tilde{\chi}(k)$, electromechanical coupling coefficient $\tilde{\eta}(k)$, and the effective elastic compliance $\tilde{\vartheta}(k)$ in k-domain on the modulation period k is rather weak. Values of $\tilde{P}$ and $\tilde{U}$ are calculated for $\tilde{E} = 0$ from Eqs.(4) and (5), respectively, and the value of the critical temperature, T_{tr}, where the transition from the paraelectric to the ferrielectric phase occurs, and where the physical properties have peculiarities, is calculated from Eq.(6).

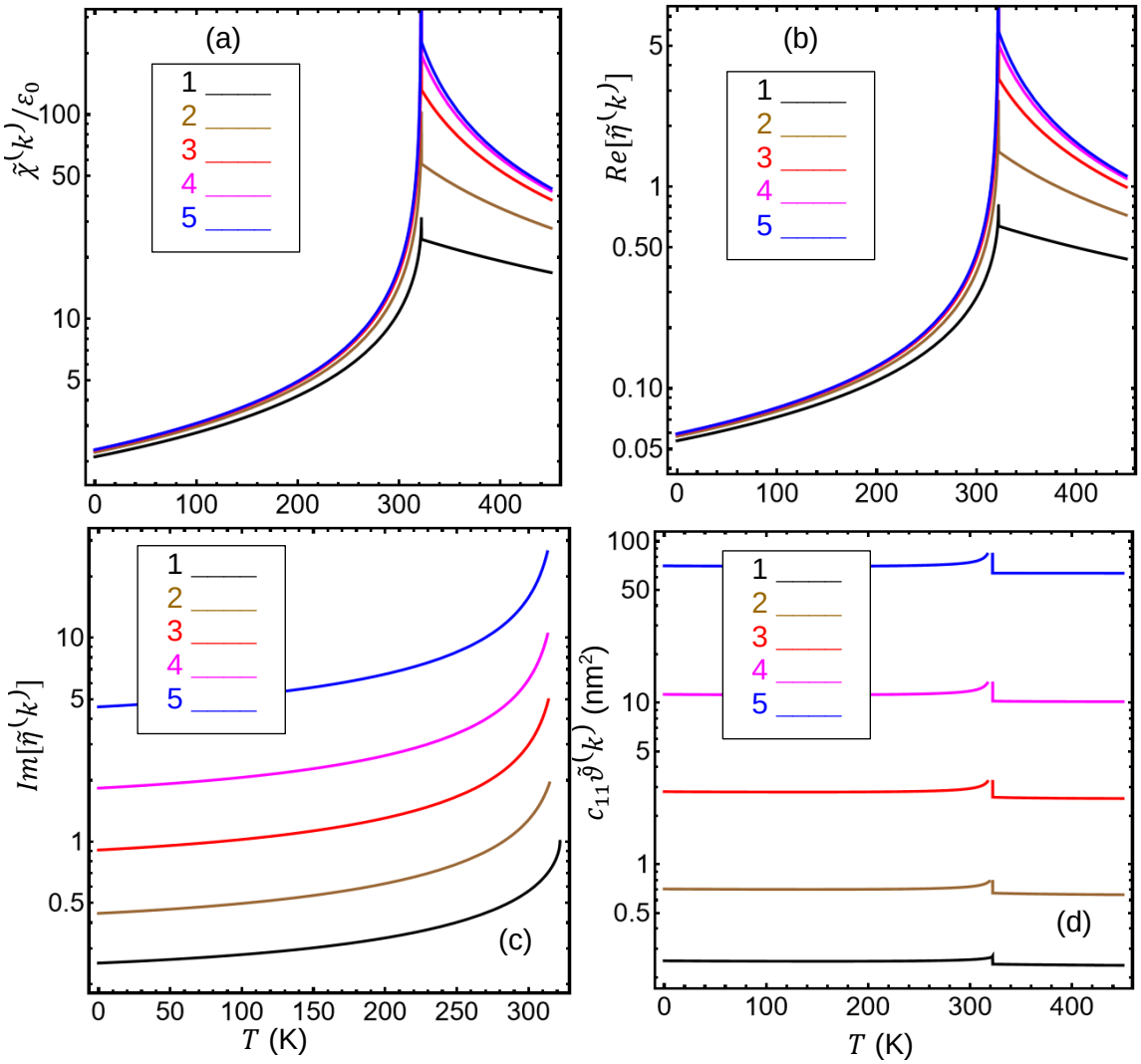

Fig. 2. Temperature dependences of the effective dielectric susceptibility $\tilde{\chi}(k)$ **(a)**, real **(b)** and imaginary **(c)** parts of the electromechanical coupling coefficient $\tilde{\eta}(k)$, and the effective elastic compliance $\tilde{\vartheta}(k)$ **(d)** calculated for several values of the stress modulation period $2\pi/k$ = 2.5, 5, 10, 25 and 50 nm (curves 1, 2, 3,4 and 5, respectively). CIPS parameters are listed in Помилка! Джерело посилання не знайдено.Part (a) is adapted from the Supplementary Materials to Ref.[12] for completeness**.**

The graph **Fig. 2** shows that the effective dielectric susceptibility $\tilde{\chi}(k)$, real parts of the electromechanical coupling coefficient $\tilde{\eta}(k)$ monotonically increase in the interval from 0 to 320 K. At the transition point, T_{tr} = 320 K, they reach the maximal value and begins to decrease slightly and monotonically. For all calculated values of the stress

modulation period $2\pi/k$ from 2.5 nm to 50 nm, the function form of the graphs is the same.

The temperature dependences of the imaginary part of the electromechanical coupling coefficient $\tilde{\eta}(k)$ represent a smooth rising lines, the function reaches its maximum value at temperature $T = T_{tr}$

The temperature dependences of the effective elastic compliance $\tilde{\vartheta}(k)$, shown in **Fig. 2d**, are parallel almost horizontal lines, which have a small jump at the transition temperature T_{tr} for all values of the k-modulation period from 2.5nm to 50 nm.

The dependences of effective dielectric susceptibility $\tilde{\chi}(k)$, real and imaginary parts of electromechanical coupling coefficient $\tilde{\eta}(k)$, and effective elastic compliance $\tilde{\vartheta}(k)$ on the temperature T and modulation period $2\pi/k$ are shown in **Fig. 3.** Here the peculiarities at $T = T_{tr}$ are clearly visible.

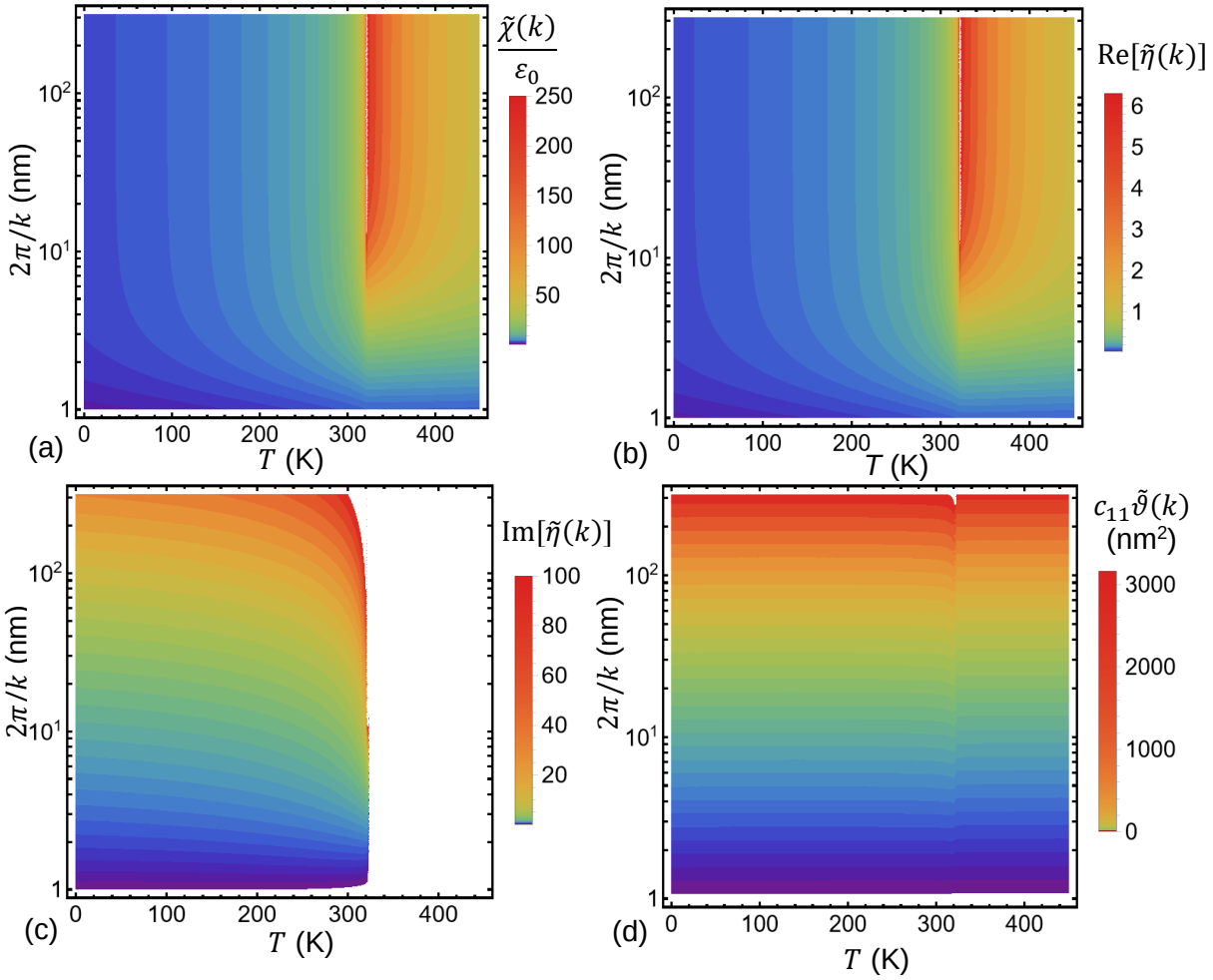

Fig. 3. The dependences of effective dielectric susceptibility $\tilde{\chi}(k)$ **(a)**, real **(b)** and imaginary **(c)** parts of electromechanical coupling coefficient $\tilde{\eta}(k)$, and effective elastic compliance $\tilde{\vartheta}(k)$ **(d)** on the temperature T and modulation period $2\pi/k$. CIPS parameters are listed in Помилка! Джерело посилання не знайдено.Part (a) is adapted from the Supplementary Materials to Ref.[12] for completeness**.**

TABLE I. LGD PARAMETERS FOR A BULK FERROELECTRIC $CuInP_2S_6$ AT FIXED STRAINS TAKEN FROM REFS.[12-14]

coefficient	***Value***
ε_b	9
α_T (C^{-2}·m J/K)	1.64067×10^7
T_C (K)	292.67
β (C^{-4}·m^{5}J)	$8.43 \cdot 10^{12}(1. - 0.00239\,T + 2.28 \cdot 10^{-6}T^2)$
γ (C^{-6}·m^{9}J)	$-1.67283 \cdot 10^{16}(1 - 0.00249\,T + 3.389 \times 10^{-6}\,T^2)$
δ (C^{-8}·m^{13}J)	$9.824 \cdot 10^{18}(1 - 0.00127\,T + 4.0999 \cdot 10^{-6}T^2)$
q_{i3} (J C^{-2}·m)	$q_{13} = 1.4879 \cdot 10^{11}(1 - 0.00206\,T)$, $q_{23} = 1.0603 \cdot 10^{11}(1 - 0.00203\,T)$, $q_{33} = -4.0334 \cdot 10^{11}(1 - 0.00188\,T)$
z_{i33} (C^{-4}·m^{5}J)	$z_{133} = -1.414 \cdot 10^{14}(1 - 0.00099\,T)$, $z_{233} = -0.774 \cdot 10^{14}(1 - 0.00146\,T)$, $z_{333} = 1.181 \cdot 10^{14}(1 - 0.00699\,T)$
s_{ij} (Pa^{-1}) c_{ij} (Pa)	$s_{11} = 1.510 \cdot 10^{-11}$, $s_{12} = 0.183 \cdot 10^{-11}$, $c_{11} = 6.803 \cdot 10^{10}$, $c_{12} = -7.364 \cdot 10^9$
g_{33ij} (J m^3/C^2)	Estimated parameter, which has an order of 10^{-9}, e.g., $g \cong$(0.5 - 2.0)×10^{-9}

III. RESULTS AND CONCLUSIONS

Using the LGD phenomenological approach we studied the strain-polarization coupling in the low-dimensional van der Waals ferrielectrics. We evolve the analytical expressions of the piezoelectric susceptibility of the material in response to the periodic strain modulation, such as caused by a SAW. Numerical calculations are performed for the vdW ferrielectric CIPS, which is a very promising candidate for advanced nanoelectronics. It was found that the dielectric susceptibility, elastic compliance and the real part of piezoelectric

susceptibility reach their maximum at the transition temperature T_{tr} = 320 K, of about 320 K. Also, the simulation results indicate a significant dependence of the studied parameters on the SAW modulation period, and this makes CIPS layers promising candidate for its application in piezoelectric and straintronic devices.

DATA AVAILABILITY STATEMENT

Numerical results presented in the work are obtained and visualized using a specialized software, Mathematica 13.2 [23]. The Mathematica notebooks, which contain the codes, are available per reasonable request.

ACKNOWLEDGMENT

A.N.M. work is supported by the Ministry of Science and Education of Ukraine (grant № PH/ 23 - 2023, "Influence of size effects on the electrophysical properties of graphene-ferroelectric nanostructures") and support from the Horizon Europe Framework Programme (HORIZON-TMA-MSCA-SE), project № 101131229, Piezoelectricity in 2D-materials: materials, modeling, and applications (PIEZO 2D).

REFERENCES

[1] K. S. *Novoselov*, A. Mishchenko, A. Carvalho, and A. H. Castro Neto, '2D materials and van der Waals heterostructures', *Science (1979)*, vol. 353, no. 6298, Jul. 2016, doi: 10.1126/science.aac9439.

[2] S. Kang *et al.*, 'Atomic-scale symmetry breaking for out-of-plane *piezoelectricity* in two-dimensional transition metal dichalcogenides', *Nano Energy*, vol. 58, pp. 57–62, Apr. 2019, doi: 10.1016/j.nanoen.2019.01.025.

[3] R. Grasset *et al.*, 'Pressure-Induced Collapse of the Charge Density Wave and Higgs Mode Visibility in 2H−TaS_2', *Phys Rev Lett*, vol. 122, no. 12, p. 127001, Mar. 2019, doi: 10.1103/PhysRevLett.122.127001.

[4] C. J. Butler *et al.*, 'Mapping polarization induced surface band bending on the Rashba semiconductor BiTeI', *Nat Commun*, vol. 5, no. 1, p. 4066, Sep. 2014, doi: 10.1038/ncomms5066.

[5] Y. Qi *et al.*, 'Topological Quantum Phase Transition and Superconductivity Induced by Pressure in the Bismuth Tellurohalide BiTeI', *Advanced Materials*, vol. 29, no. 18, p. 1605965, May 2017, doi: 10.1002/adma.201605965.

[6] L. Dong, J. Lou, and V. B. Shenoy, 'Large In-Plane and Vertical Piezoelectricity in Janus Transition Metal Dichalchogenides', *ACS Nano*, vol. 11, no. 8, pp. 8242–8248, Aug. 2017, doi: 10.1021/acsnano.7b03313.

[7] S. Zhou, L. You, H. Zhou, Y. Pu, Z. Gui, and J. Wang, 'Van der Waals layered ferroelectric CuInP2S6: Physical properties and device applications', *Front Phys (Beijing)*, vol. 16, no. 1, p. 13301, Feb. 2021, doi: 10.1007/s11467-020-0986-0.

[8] F. Liu *et al.*, 'Room-temperature ferroelectricity in CuInP2S6 ultrathin flakes', *Nat Commun*, vol. 7, no. 1, p. 12357, Aug. 2016, doi: 10.1038/ncomms12357.

[9] S. M. Neumayer *et al.*, 'The Concept of Negative Capacitance in Ionically Conductive Van der Waals Ferroelectrics', *Adv Energy Mater*, vol. 10, no. 39, Oct. 2020, doi: 10.1002/aenm.202001726.

[10] X. Jiang *et al.*, 'Ferroelectric Field-Effect Transistors Based on WSe_2 /$CuInP_2S_6$ Heterostructures for Memory Applications', *ACS Appl Electron Mater*, vol. 3, no. 11, pp. 4711–4717, Nov. 2021, doi: 10.1021/acsaelm.1c00492.

[11] M. Si, P.-Y. Liao, G. Qiu, Y. Duan, and P. D. Ye, 'Ferroelectric Field-Effect Transistors Based on MoS_2 and $CuInP_2S_6$ Two-Dimensional van der Waals Heterostructure', *ACS Nano*, vol. 12, no. 7, pp. 6700–6705, Jul. 2018, doi: 10.1021/acsnano.8b01810.

[12] Y. Liu, A. N. Morozovska, A. Ghosh, K. P. Kelley, E. A. Eliseev, J. Yao, Y. Liu, and S. V. Kalinin, Disentangling stress and curvature effects in layered 2D ferroelectric $CuInP_2S_6$. ASC Nano, **17**, № 21, 22004–22014 (2023), https://doi.org/10.1021/acsnano.3c08603

[13] A. N. Morozovska, E. A. Eliseev, Y. Liu, K. P. Kelley, A. Ghosh, Y. Liu, J. Yao, N. V. Morozovsky, A. L Kholkin, Y. M. Vysochanskii, and S. V. Kalinin. Bending-induced isostructural transitions in ultrathin layers of van der Waals ferrielectrics. Acta Materialia, **263**, 119519 (2024), https://doi.org/10.1016/j.actamat.2023.119519

[14] A. N. Morozovska, E. A. Eliseev, L. P. Yurchenko, V. V. Laguta, Y. Liu, Sergei V. Kalinin, A. L Kholkin, and Y. M. Vysochanskii. The strain-induced transitions of the piezoelectric, pyroelectric and electrocaloric properties of the $CuInP_2S_6$ films, AIP Advances **13**, 125306 (2023), https://doi.org/10.1063/5.0178854.

[15] W. F. Io *et al.*, 'Strong piezoelectric response in layered CuInP2S6 nanosheets for piezoelectric nanogenerators', *Nano Energy*, vol. 99, p. 107371, Aug. 2022, doi: 10.1016/j.nanoen.2022.107371.

[16] M. Si *et al.*, 'Room-Temperature Electrocaloric Effect in Layered Ferroelectric $CuInP_2S_6$ for Solid-State Refrigeration', *ACS Nano*, vol. 13, no. 8, pp. 8760–8765, Aug. 2019, doi: 10.1021/acsnano.9b01491.

[17] Y. Liu *et al.*, 'Stress and Curvature Effects in Layered 2D Ferroelectric $CuInP_2S_6$', *ACS Nano*, vol. 17, no. 21, pp. 22004–22014, Nov. 2023, doi: 10.1021/acsnano.3c08603.

[18] V V. Samulionis, J. Banys, and Yu. Vysochanskii, 'Linear and Nonlinear Elastic Properties of $CuInP_2S_6$ Layered Crystals Under Polarization Reversal', *Ferroelectrics*, vol. 389, no. 1, pp. 18–24, Oct. 2009, doi: 10.1080/00150190902987459.

[19] A. N. Morozovska, M. D. Glinchuk, E. A. Eliseev, and Y. M. Vysochanskii. Flexocoupling-induced soft acoustic mode and the spatially modulated phases in ferroelectrics. Physical Review **B**, 96, 094111 (2017) doi/10.1103/PhysRevB.96.094111

[20]. L. D. Landau and E. M. Lifshitz, *Theory of Elasticity*, vol. 7. Oxford, U.K.: Elsevier, 1986. doi: 10.1016/C2009-0-25521-8.

[21] G. A. Smolenskii, V. A. Bokov, V. A. Isupov, N. N. Krainik, R. E. Pasynkov, and A. I. Sokolov, *Ferroelectrics and Related Materials*. New York: Gordon and Breach, 1984.

[22] B. A. Strukov and A. P. Levanyuk, *Ferroelectric Phenomena in Crystals: Physical Foundations*, 1st ed. Berlin, Heidelberg: Springer Berlin Heidelberg, 1998. doi: 10.1007/978-3-642-60293-1.

[23] 'Wolfram Mathematica: Modern Technical Computing'. Accessed: Jan. 08, 2024. [Online]. Available: https://www.wolfram.com/mathematica/.